Fusion Engineering and Design 194 (2023) 113745

Contents lists available at ScienceDirect

Fusion Engineering and Design

journal homepage: www.elsevier.com/locate/fusengdes

Frequency response analysis of a toroidal field coil of the divertor tokamak test facility

G. Messina [a,c,*], R.C. Lopes [b], P. Zito [a,c], L. Morici [a,c], A. Di Zenobio [a,c], G. Ramogida [a,c]

[a] Superconductivity Section, FSN Department, ENEA, Italy
[b] Department of Engineering, University of Palermo, Italy
[c] DTT S.c.a r.l., c/o ENEA, Italy

ARTICLE INFO

Keywords:
Resonance frequency
CICC (cable in conduit conductor)
Superconducting magnets
Lumped network

ABSTRACT

The magnet system of the Divertor Tokamak Test (DTT) facility is mainly made up with superconducting coils. During the operation of the DTT machine, high voltages will appear across each Toroidal Field Coil (TFC) when fast current will ramp down; the reason why, a reliable electrical insulation is required for the operation of the TFC system. With the aim of checking the correct sizing and implementation of the electrical insulation, different DC and AC electrical tests will be performed during all the coil manufacturing process. Among these, the impedance spectrum test, or rather the complex impedance measurement over several decades of frequency range, can be used to analyze the frequency response of the coil. The variations of the resonance frequency (f_0), during its electrical acceptance test, can be useful to make predictions about the detectability of internal failure conditions in a coil. This paper focuses on analysis of the frequency response of a TFC, using a numerical simulation approach. The goal is to assess the impedance spectrum of a TFC within a fixed frequency band by a frequency-dependent lumped network. Starting from the TFC layout, a WP with the casing has been modeled by a complex network of lumped parameters in Ansys 2021/R2 environment. The data (amplitude and phase angle vs frequency) obtained have been used to study the f_0 variation during the different manufacturing stage of the WP. This model will be able to make predictions about the detectability of internal short-circuit in a TFC.

1. Introduction

With the aim to explore different divertor solutions for power and particles exhaust, a Divertor Tokamak Test facility (DTT) is under construction at ENEA Research Centre in Frascati (Italy) [1,2]. The DTT magnet system is made up with superconducting coils due to the required intense magnetic fields. In particular, the TFCs system consists of: 18 coils connected in series and three Fast Discharge Units (FDUs), each of which drives a group of 6 TFCs. The FDU is a key component for the protection of the magnets as it allows the rapid discharge of the magnets in case of a quench or of a fault. An overvoltage will appear across each TFC when a current will ramp down for a fast safety discharge, so that a reliable electrical insulation for each TF coil is mandatory [3–5]. Therefore, in the complex design procedure, it has been paid attention to the guidelines for a good high voltage insulation. Each of the TFC can be thought as a parallel RLC circuit where, at the f_0, the susceptance (the imaginary term of admittance) becomes zero. When this occurs, the coil admittance, Y_{coil}, has only the real term. Therefore, at the resonance, the coil impendence, Z_{coil}, is maximum and decreases at lower and higher frequencies. If a fault condition occurs inside the coil, the inductance value changes and, consequently, also the f_0 value changes from its starting value. This situation causes a shift of the Z_{coil} versus f curve. With the aim of checking the correct sizing and implementation of the electrical insulation, different DC and AC electrical tests will be performed during all the coil manufacturing process (both on the WP manufacturing and on the integration into case). Among these, the impedance spectrum test, or rather the complex impedance measurement over several decades of frequency range, can be used to analyze the frequency response of the coil. The variations of the f_0 parameter during its electrical acceptance test, can be useful to make predictions about the detectability of internal failure conditions (short-circuit, ground fault, and so on) in a coil. A variation of the frequency across the f_0 indeed, provides a higher sensitivity for short circuits detection inside the TFC, for example [6–8]. Such short circuits could be caused by an insufficient/degradation insulation in the crossing point of two conductors or between a conductor and the ground or by an

* Corresponding author.
E-mail address: giuseppe.messina.fra@enea.it (G. Messina).

https://doi.org/10.1016/j.fusengdes.2023.113745
Received 11 October 2022; Received in revised form 5 April 2023; Accepted 11 April 2023
Available online 14 April 2023

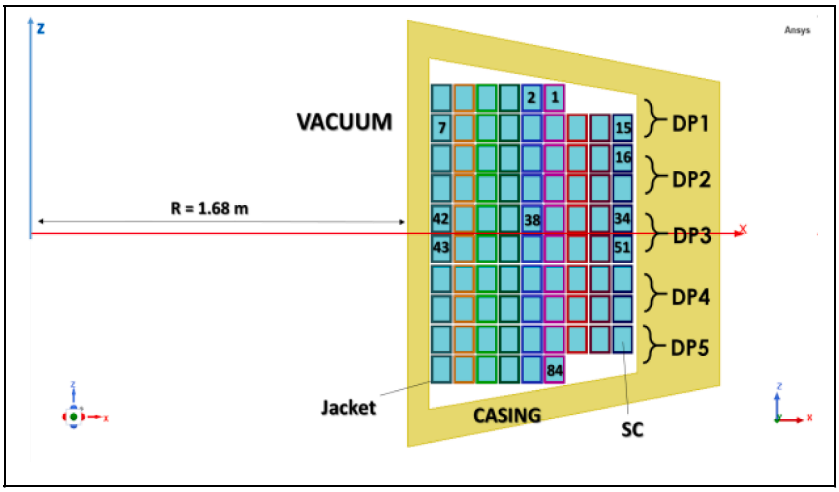

Fig. 1. Axisymmetric 2D model of the TFC in *Ansys Maxwell*.

Table I
Electrical Conductivity (S/m) @ cryogenic temperature.

Domain	Material	Value
Casing	Stainless-steel	1.88×10^{6}
SC	LTS	1×10^{12}
Jacket	Stainless-steel	1.88×10^{6}
Vacuum	Air	0

inappropriate pressure during vacuum impregnation, and so on. Because the eddy currents in the casing can mask a short circuit when the WP has been already inserted into it, modeling is important to check the detection limits of the test. The simulation studies described in this paper are based on appropriate electrical circuits, developed, and suited for the DTT TFC design characteristics in different production stages. The investigation analysis of the transient behavior of a TFC has been started with the calculation of f_0 in the frequency domain. Starting from the TFC geometry, a CAD model has been drawn into *Ansys SpaceClaim* and then exported into *Ansys Maxwell*. After a convenient choice of the materials, a Finite Element Methods (FEM) calculations have been carried out to estimate the frequency dependent electrical resistances and the inductances matrix of the overall TFC. The overall TFC is made up of the WP and the casing. The TFC matrix has been imported in *Ansys Simplorer* as a coupling matrix and connected to the analytically estimated capacitances matrix. Therefore, a complex network of frequency dependent lumped parameters has been assembled for a TFC, considering more than one electric element (R, L, M and C); each turn of the WP and the casing has been considered. Suitable parameters have also been introduced in the TFC circuital model to estimate the impedance spectrum for different case studies: *case study 1* for the WP without conductive paint layer [9–10]; *case study 2* for the WP with conductive paint layer; *case study 3* for the WP electrically insulated and assembled into stainless steel casing; *case study 4* for the TFC (WP + casing) with short circuit at terminals of different Double Pancakes (DPs); *case study 5* for the TFC (WP + casing) with a ground fault at one terminal of different DPs.

2. TFC geometry discretization

The 84 turns of the D-shaped TFC have been subdivided into five DPs. The outermost DPs have 15 turns, while each of the innermost DPs has 18 turns. The superconducting CICC, used to wind the TFC, is made

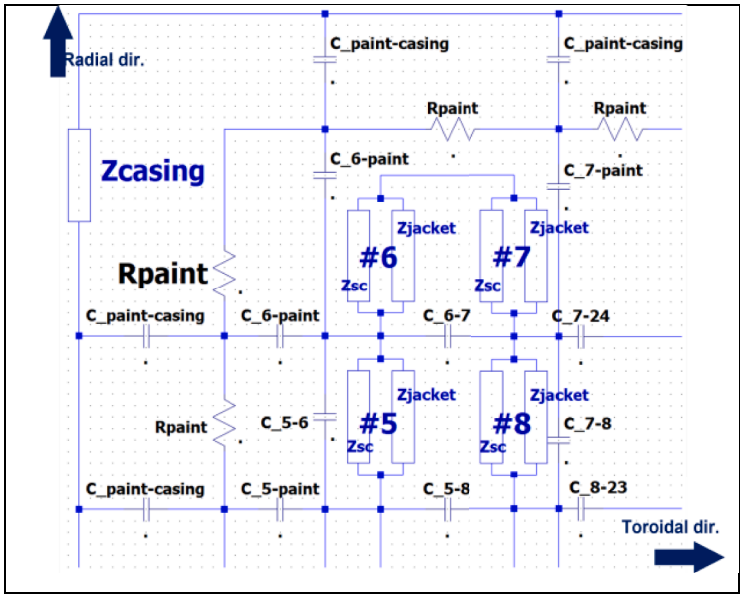

Fig. 2. Simplified circuital configuration of some turns (#) of a TFC.

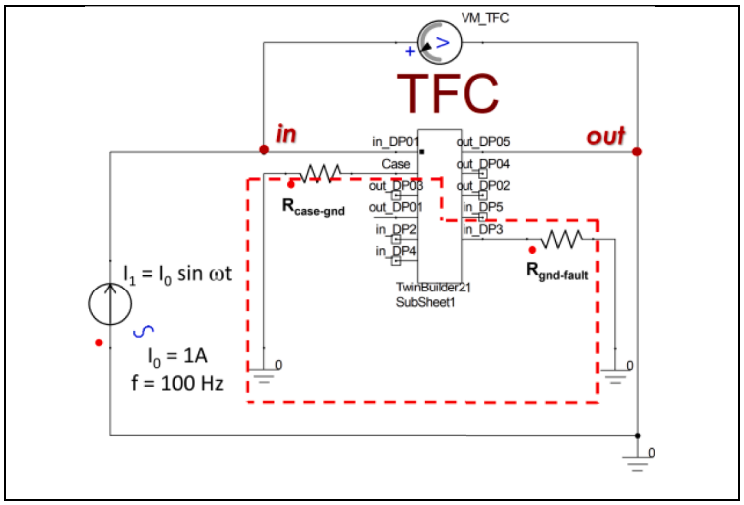

Fig. 3. Electrical circuit used to investigate the transient behavior of a TFC.

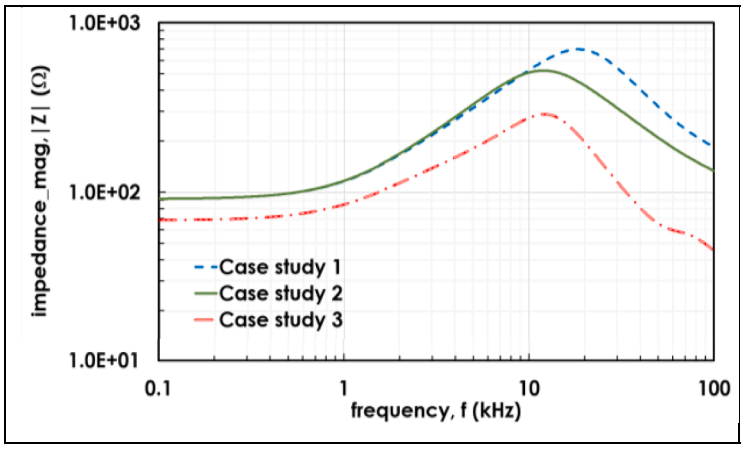

4a

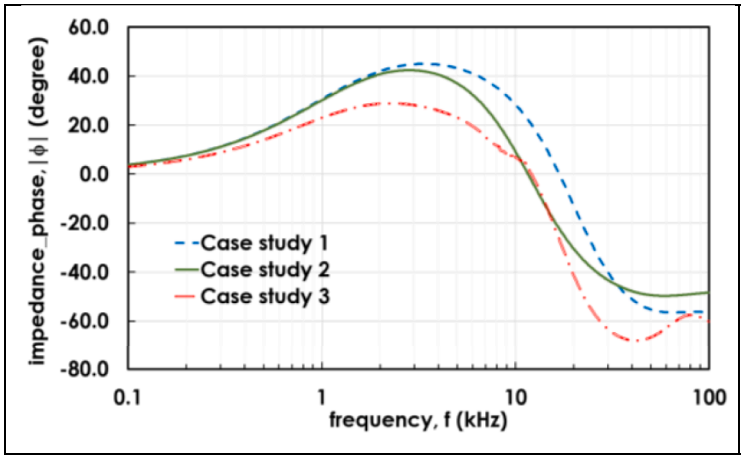

4b

Fig. 4. a. Impedance data computed for the *case studies 1-3*.
b. Phase angle data computed for the *case studies 1-3*.

of a cable enclosed in a stainless-steel jacket with a rectangular cross section and a thickness of 2 mm. The CICC is surrounded by an insulation made of a fiberglass tape; the thickness of the electrical insulation between adjacent conductors is 2 mm. An additional 0.5 mm-thick fiberglass tape is interposed between adjacent double pancakes. The complete WP is wrapped by a 2 mm thickness alternate fiberglass/polyamide layer insulation, with a further layer of conductive paint deposited on its outer surface. Its role is to homogenize the electrical field on the outer surface of the coil. The WP is enclosed in a stainless-steel casing and the remaining void space between them is filled by

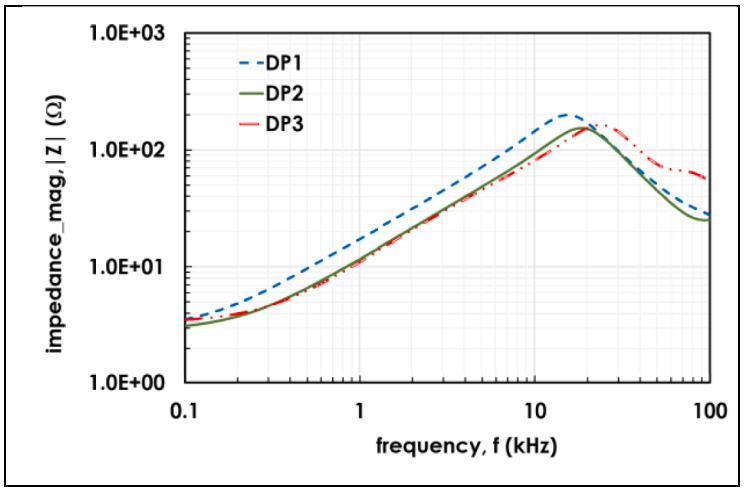

5a

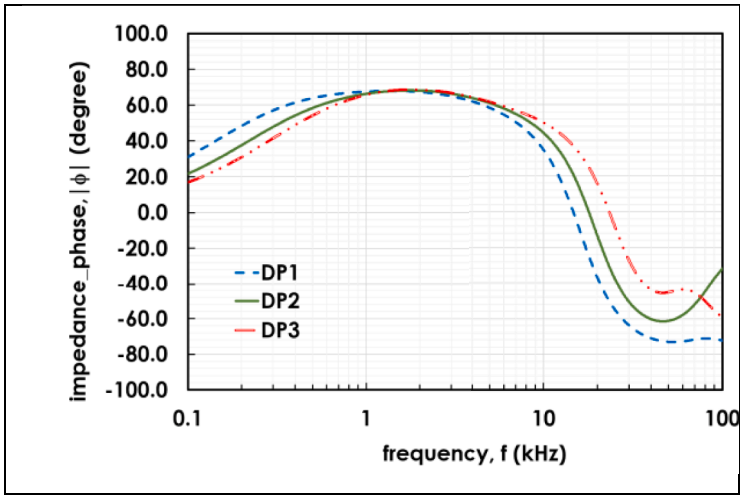

5b

Fig. 5. a. Impedance data computed for the *case study 4*: a short circuit occurs at terminals of different DPs.
b. Phase angle data computed for the *case study 4*: a short circuit occurs at terminals of different DPs.

fiberglass. After all these operations, all the magnet is filled by epoxy resin by a Vacuum Pressure Impregnation process and then cured, in order to obtain the final G10 insulation. In order to model each turn of the WP, the D-shaped TFC (which geometric dimensions are: TFC height ≈ 6 m; TFC width ≈ 3.2 m) is approximated by a circularly shaped TFC having the same self-inductance. An internal radius of R= 1.68 m is estimated, and the same casing and WP cross-section has been adopted. Even if the magnetic field of a D-shaped TF is different from that of a circular one having the same self-inductance being the aim of the simulation the inductance coefficients matrix extraction, this is acceptable. The preliminary magneto-static analysis on this simplified model coil returned a self-induction coefficient, (L_C= 46.6 mH), only 2% different from that of the D-shaped coil (L_D= 45.71 mH). Taking this into account, a 2D axisymmetric FEM model has been implemented in *Ansys Maxwell* and described in the following section.

3. FEM model of a TFC

To develop a frequency-dependent lumped network, a 2D axisymmetric FEM model of the cross section of a TFC has been implemented in *Ansys Maxwell* (Fig. 1) [11,12]. The TFC model, composed of the 84 turns of the WP and the casing, has been divided into four domains: Casing, Superconductor (SC), Jacket, Vacuum. Each domain is associated to a material, chosen from those of the *Ansys Maxwell* library, whose electrical conductivity value at cryogenic temperature has been reported in Table I.

Setting a magneto-static analysis and an eddy current analysis in the frequency range 0.1 Hz ÷ 100 kHz, the resistances, the self- and mutual inductance coefficients of each turn and of the casing have been computed. This 169 × 169 matrix (84 SC, 84 jackets, 1 casing) of frequency dependent parameters has been exported into *Ansys Simplorer* as coupling matrix. Eddy current calculation has been set only on the jacket and casing domains while the resistance of the superconducting material, $R_{SC,}$ has been supposed to be frequency independent. A negligibly small (non-zero) value has been assigned to it, for computational purposes. The self and mutual inductances of the turns of a TFC decrease with increasing frequency due to the eddy currents induced in the stainless-steel jacket of the conductor [13].

4. AC modeling by lumped network

To estimate the impedance spectrum of a TFC for different the *case studies*, a frequency-dependent lumped network has been assembled in *Ansys Simplorer* environment. The element of the matrix associated to each turn and casing is a box with a total of 169 pair of electric ports, connected according to the geometry and the winding sequence. Fig. 2

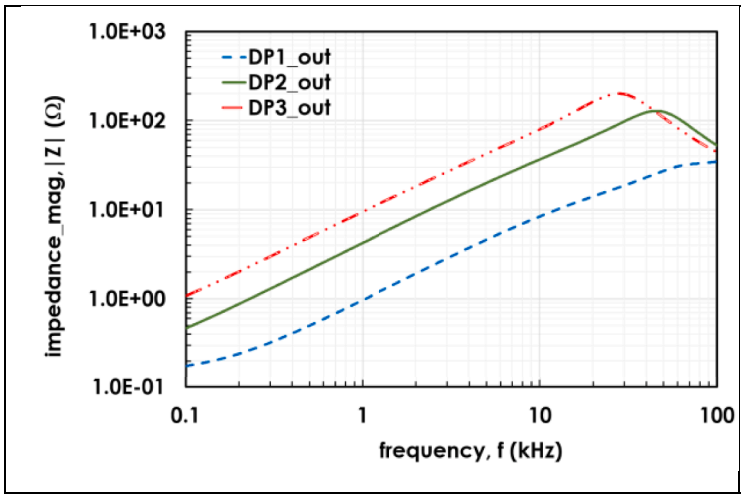

6a

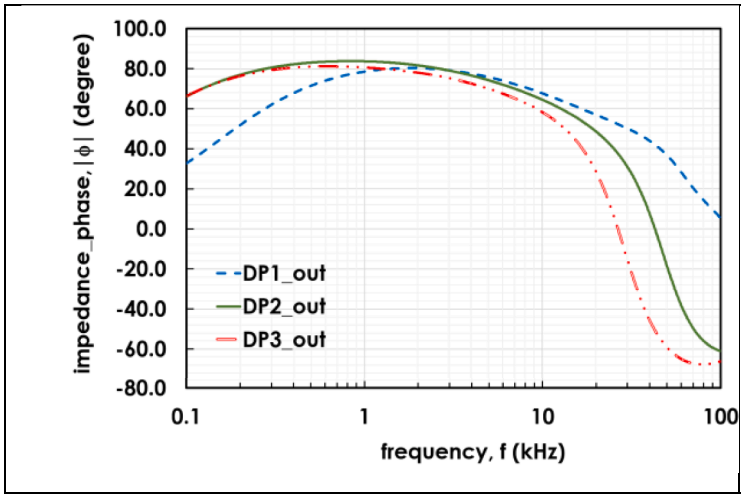

6b

Fig. 6. a. Impedance data computed for the *case study 5*: a ground fault at one terminal of a DP.
b. Phase angle data computed for the *case study 5*: a ground fault at one terminal of a DP.

qualitatively describes the electrical circuit associated to each single turn: two impedances (Z_{SC} and Z_{jacket}) connected in parallel and coupled magnetically, the inter-turn capacitances in both radial (*x*-axis) and toroidal (*z*-axis) direction, the capacitances between the outer turns to grounded parts. All capacitances are frequency-independent and have been estimated analytically in both toroidal (C_{tor}) and radial direction (C_{rad}); the formulas of parallel plate capacitor and the cylindrical capacitor has been applied, respectively [14]. The range of the capacitance values is a function of the location of the turns and of the outermost turns with respect to the conductive paint layer and is reported in Ref. [3]. The lumped network associated to a TFC is modeled as the sub-circuit shown in Fig. 3. This sub-circuit has 5 pairs of terminals *IN* and *OUT* (one pair for each DP) plus the casing terminal. It also includes: the joint resistances ($R_{joint} = 5$ nΩ) connecting adjacent DPs; the R_{paint}= 8 kΩ is the total resistance value of the conductive paint layer, applied on the external surface of the coil. In our model, this value has been subdivided into 38 sections (as many as the capacitances between each turn and the paint layer in both directions), each one having a resistance of 210 Ω [3].

Starting from the circuital models show in Figs. 2 and 3, different parameters and configurations have been used to estimate the impedance spectrum of the coil in different stages of its manufacturing process. For the *case study 1* and the *case study 2* the WP without and with conductive paint, respectively, has been analyzed, while the casing effects have not been considered. In the first case, TFC behavior is studied considering the resistance and the inductance matrix plus the network of all capacitances between adjacent turns in both directions. In the *case study 2*, R_{paint}, $C_{turn\text{-}paint,tor}$ and $C_{turn\text{-}paint,rad}$ parameters have been inserted into the TFC electrical circuit to model the conductive paint applied on the outer surface of the WP. The frequency-dependent electrical parameters of the casing (resistance, self- and mutual inductances) have been inserted into the circuital model (*case study 3*) when the coil manufacturing process is completed by inserting the WP into the casing. The conductive paint and casing have been electrically connected among each other and then connected to ground by a resistance of 0.1 Ω. The *case study 4* investigates the short-circuit influence on f_0. A resistance ($R_{short\text{-}circuit} = 1$ pΩ) has been included in the circuital model to simulate an ideal short circuit in different locations of the WP: at DP1, DP2 and DP3 terminals. Finally, a fault ground across one terminal of different DPs has been analyzed for the *case study 5*: the impedance spectrum of the TFC has been computed for a ground fault resistance value of $R_{fault\_gnd} = 1$ pΩ connected to DP1, DP2 or DP3 terminal.

5. Simulation results

Setting an AC decade sweep-type with 1000 points sensibility, an AC analysis has been carried out in the 100 Hz ÷ 100 kHz frequency range. Figs. 4a and 4b show the impedance spectrum results corresponding to the circuital model used for the *case studies 1, 2* and *3*. The spectrum of WP without conductive paint has a smoothed resonance at a frequency around f_0= 16.9 kHz, because the model can estimate the damping caused by the skin effect in the jacket. When a conductive paint layer is applied on a WP insulation surface, the resonance shifts to a lower frequency value, f_0= 11.6 kHz, due to the resistance of the conductive paint plus the additional capacitances. In the case study 3, the main effect of the casing can be observed: it acts as a secondary winding of a transformer whose primary is the WP. Therefore, inserting the WP into the casing, both a reduction of the maximum value of $|Z|$ of almost 50% (with respect to the *case study 2*) and a slightly increase in f_0 can be estimated. For case studies 1, 2 and 3, the $|Z|_{max}$ and f_0 value are, respectively: 696 Ω and 16.9 kHz; 522 Ω and 11.6 kHz; 288 Ω and 12.1 kHz.

Figs. 5a and 5b show the impedance and phase angle data, respectively, computed for the *case study 4*. With reference to the impedance spectrum of an undamaged coil (*case study 3* of Figs. 4a and 4b), and assuming that only variations of the impedance larger than 10% are reliably detectable, it is possible to conclude that ideal short circuits ($R_{short\text{-}circuit}$ almost zero) like those investigated across DP1 ($|Z|_{max} = 198$ Ω, $f_0 = 14.9$ kHz), DP2 ($|Z|_{max} = 151$ Ω, $f_0 = 17.9$ kHz) and DP3 ($|Z|_{max} = 164$ Ω, $f_0 = 23.4$ kHz), are detectable.

The *case study 5* results are shown in Fig. 6a and 6b: moving from the outermost to the central DP, a 70% decrease of the f_0 value and a $|Z|_{max}$ value increase of about one order magnitude can be observed (DP1 has $|Z|_{max} < 34$ Ω, $f_0 > 100$ kHz; DP2 has $|Z|_{max} = 122$ Ω, $f_0 = 43.6$ kHz; DP3 has $|Z|_{max} = 197$ Ω, $f_0 = 27$ kHz). This result can be associated to an increase of the fault circuit impedance value (red dashed line in the Fig. 3) when, moving from DP1 to DP3, a ground fault bypasses a lower number of WP sections.

6. Conclusions

TFC impedance magnitude and phase angle have been computed for a 3-decade frequency spectrum. The spectrum of a bare WP without conductive paint layer has a very sharp resonance. This resonance shifts to a lower frequency when a conductive paint layer is applied to the outer surface of the WP, while a slight increase is observed when the WP is inserted in the stainless-steel casing. Starting from the obtained value for an undamaged coil, a shift of f_0 has been observed on the coil impedance spectrum when an ideal short-circuit in different DPs, inside of the WP, has been simulated. Moving from the outermost to the central DP, the short circuit generates a resonance shift to a higher frequency, while the impedance value shifts to lower values. The estimated impedance spectrum for a ground fault at one terminal of different DPs shows an opposite trend to the short-circuit case both for the f_0 and the maximum impedance value. The results suggest that the impedance spectrum test is a quick and reliable technique; knowing the f_0 of an undamaged coil, it can be employed as tool to detect a failure accidentally created during the various manufacturing stages of a TFC.

Declaration of Competing Interest

The authors declare that they have no known competing financial interests or personal relationships that could have appeared to influence the work reported in this paper.

Data availability

No data was used for the research described in the article.

Acknowledgments

This contribution is part of a set of papers (3 Invited Talks, some oral presentations, and a few dozen posters) presented at SOFT Dubrovnik to illustrate the state of implementation of the DTT program. The DTT Team will be happy to provide any further information; please contact info@dtt-project.it

References

[1] DTT Divertor Tokamak Test facility Interim Design Report, in: R. Martone, R. Albanese, F. Crisanti, A. Pizzuto, P. Martin (Eds.), ENEA, ("Green Book"), April 2019 (ISBN 978-88-8286-378-4).
[2] R. Ambrosino, DTT - divertor tokamak test facility: a testbed for DEMO, Fusion Eng. Des. 167 (2021), 112330.
[3] G. Messina, et al., Transient electrical behavior of the TF superconducting coils of divertor tokamak test facility during a fast discharge, IEEE TAS 32 (Jun. 2022), 4901610. Art. no.
[4] R. Wesche, X. Sarasola, R. Guarino, K. Sedlak, P. Bruzzone, Parametric study of the TF coil design for the European DEMO, Fusion Eng. Des. 164 (2021), 112217.
[5] S. Fink, T. Bonicelli, W.H. Fietz, A. Miri, X. Quanc, A. Ulbricht, Transient electrical behaviour of the ITER TF coils during fast discharge and two fault cases, Fusion Eng. Des. 75-79 (2005) 135–138.
[6] H. Ehmler, et al., Comparative analysis of impulse and impedance tests to detect short circuits within the W7-X Magnets, IEEE TAS 16 (Jun. 2006) 767–770.
[7] K. Rißе, et al., Design, tests and repair procedures for the electrical insulation of the superconducting W7-X magnets, IEEE TAS 20 (Apr. 2010) 447–450.
[8] A. Bruno, et al., Broadband electromagnetic modeling of the superconducting toroidal field magnets of JT-60SA: transient simulation and fault detectability, IEEE TAS 27 (Aug. 2017), 4201608. Art. no.
[9] A. Di Zenobio, et al., DTT device: conceptual design of superconducting magnet system, Fusion Eng. Des. 146 (Apr 2017) 299–312.
[10] H. Ehmler, M. Köppen, ac modeling and impedance spectrum tests of the superconducting magnetic field coils for the Wendelstein 7-X fusion experiment, Rev. Sci. Instrum. 78 (Oct 2007), 104705. Art. no.
[11] A. Bruno, et al., Broadband electromagnetic modeling of the superconducting toroidal field magnets of JT-60SA: transient simulation and fault detectability, IEEE TAS 27 (Aug. 2017), 4201608. Art. no.
[12] A.M. Miri, et al., Transient behavior of superconducting magnet systems of fusion reactor ITER during safety discharge, *Modelling and Simulation in Engineering*, Vol. 2008 (Dec 2008). Art. ID 359210.
[13] A. Winkler, S. Fink, W.H. Fietz, M. Noe, Calculation of transient electrical behaviour of ITER PF coils, Fusion Eng. Des. 84 (Jun. 2009) 1979–1981.
[14] P. Zito, et al., Conceptual design and modeling of the toroidal field coils circuit of DTT, in: 20th *IEEE Mediterranean Electrotechnical Conference, MELECON*, Jul. 2020.